N-Terminal Modifications Increase the Neutral-pH Stability of Pepsin†

Brian C. Bryksa, Takuji Tanaka, and Rickey Y. Yada*

Department of Food Science, University of Guelph, Guelph, Ontario N1G 2W1, Canada

Received May 16, 2003; Revised Manuscript Received July 22, 2003

ABSTRACT: A structure−function study was undertaken to determine the effects of N-terminal mutations in pepsin designed to introduce the Lys-X-Tyr motif and increase N-terminal flexibility. At pH 7.0, E7K/T12A/E13Q pepsin was inactivated more slowly compared to WT, whereas the mutants E7K and T12A/E13Q were not stabilized. Far-UV circular dichroism revealed that changes in secondary structure accompanied the inactivation process, and that the structural changes occurred at approximately the same rate as inactivation. All of the inactivated pepsin forms showed retention of substantial secondary structure, more than previously determined for pepsin denatured at pH 7.2 and 8.0, suggesting the presence of a structural intermediate at pH 7.0. The coupled mutations at positions 12 and 13 impacted the pH dependence of activity at pH 0.9, lowered affinity for a synthetic substrate, and lowered the turnover number. The introduction of Lys at position 7 apparently destabilized the interaction between prosegment-enzyme body as evidenced by activation at higher pH ($\geq$ 4.0) compared to WT, but showed no change for pH dependence of activity, nor a statistically significant change in affinity for the synthetic substrate.

Pepsin is a monomeric enzyme belonging to the aspartic proteinase family that is synthesized as a zymogen in the epithelial cells lining the stomach (*1*). Upon secretion into the acidic environment of the lumen, the zymogen (pepsinogen) undergoes a series of conformational changes accompanied by self-cleavage of the prosegment, resulting in the active, mature form of the enzyme (*2*). Pepsinogen and its mature form, pepsin, differ in primary sequence by 44 amino acid residues at the N-terminus of the zymogen that are removed upon activation. The pepsin portion of the zymogen contains 327 amino acids (*3*), and like all mammalian aspartic proteinases, it is a bilobal monomer, containing an approximate 2-fold axis of symmetry between two β-sheet domains (*4*). The prosegment covers the active site thereby restricting substrate access and rendering the zymogen inactive. Hydrogen bonds between the prosegment and enzyme body are formed between polar residues of the prosegment and main-chain or side-chain atoms of the pepsin (nonprosegment) moiety (*3*). In the zymogen, residues 1p−10p of the 44-residue prosegment form the first strand of a six-stranded β-sheet. The following hydrogen-bond pairs between strands 5 and 6 of the six-stranded β-sheet were deduced from the crystal structure of pepsinogen: Val2p−Leu167, Val4p−Val165, and Leu6p−Ser163 (*3*). Also, Val7p and Lys9p have a β-sheet interaction with Phe15 and Glu13, respectively. The N-terminal region of the prosegment plays an equivalent structural role to the N-terminus of the mature enzyme comprising the first strand of a six-stranded interdomain β-sheet (*3*). The remainder of the prosegment, together with the first 13 residues of the pepsin portion of pepsinogen (residues 9p−13), takes the shape of a flattened disk that fits into the substrate-binding cleft (*2*). Arg13p forms a hydrogen bond ion pair with Asp11, and similarly Arg8p and Glu13 interact, serving to tie down the N-terminus of the zymogen.

Unlike its zymogen precursor, pepsin is irreversibly denatured at neutral pH (*5*). A stability study of the individually expressed lobes of pepsin revealed that the N-terminal lobe was selectively denatured at pH 8.0 (*6*). Five residues, Asp11, Asp159, Glu4, Glu13, and Asp118, were implicated as potentially important to the denaturation process due to electrostatic repulsion within the structure upon deprotonation of side-chain carboxyl groups (*6*). Tanaka and Yada (*7*) showed that denaturation of the N-terminal portion of pepsin initiated inactivation at neutral pH and that stabilizing the N-terminus in its native position inhibited the inactivation process (*7*).

Cathepsin D exhibits unusually high neutral pH-stability compared to most aspartic proteinases and a crystallographic study revealed the structural mode of stabilization (*8*). The pH 7.5 structure of cathepsin D revealed that the N-terminus had relocated to the active site by a 180° rotation where it was bound via a salt-bridge between Lys8 and the catalytic Asp residues (*8*). It was also observed that Ala13 functioned as a hinge point for rotation of the N-terminus into the active site. It was suggested that the Lys-X-Tyr motif of the cathepsin D N-terminus played the role of prosegment residues Lys36p and Tyr9 (pepsin numbering) in the aspartic proteinase zymogens (*8*).

Structure−function relationships observed in nature can serve as a template for the design of mutant enzymes engineered to contain a desired function. To explore the ability to transfer pH-stabilizing technology among aspartic proteinases, the present study sought to engineer a pepsin form that displayed neutral pH stability through the introduction of the cathepsin D N-terminal structural motif Lys-X-

† The financial support of the Natural Sciences and Engineering Research Council of Canada is gratefully acknowledged.

* To whom correspondence should be addressed. Fax: +1-519-824-0847; Phone: +1-519-824-4120 ext 58915; E-mail: ryada@uoguelph.ca.

10.1021/bi0348112 CCC: $25.00
Published on Web 10/25/2003

Tyr. Upon comparison of the N-terminal sequences of the pepsin and cathepsin D, three mutations were designed: Lys was incorporated at position 7 (equivalent to position 8 of cathepsin D) in place of Glu. Lys at position 7 was to provide for the formation of a salt-bridge with the catalytic Asp residues, as observed in cathepsin D. Thr12, the positional equivalent to Ala13 in cathepsin D, was replaced with Ala to provide a hinge point for rotation of the N-terminus into the active site. Last, Glu13, equivalent to Gln14 in cathepsin D, was changed to Gln to avoid charge−charge repulsion with other carboxyl groups ionized at neutral pH, potentially inhibiting the 180° rotation about the hinge point. The mutations were located as follows: E7K is part of the reverse turn, and Glu7 normally interacts via a hydrogen bond pair with Phe15 of the neighboring sheet. T12A is part of the loop within the reverse turn that connects the sixth strand of the interdomain β-sheet with the first strand of a neighboring sheet (*9*). The Thr12 side-chain shares a hydrogen bond with the main-chain carbonyl group of Leu10 (*1*). E13Q occupies the last position of the same reverse turn. In wild-type, Glu13 shares a β-sheet interaction with Tyr9, the first residue of the reverse turn (*1*, *9*).

MATERIALS AND METHODS

Materials. The plasmid containing thioredoxin-pepsinogen fusion gene, pTFP1000,[1] was utilized (*10*). The plasmid pTrueBlue was purchased from Genomics One Corp. (Laval, QC, Canada). All restriction enzymes used for plasmid manipulation were from New England Biolabs Ltd. (Mississauga, ON, Canada) or Roche Diagnostics (Laval, QC, Canada). QIAquick Gel Extraction kit and QIAquick Nucleotide Removal kit were from Qiagen Inc. (Mississauga, ON, Canada). Pfu Turbo DNA polymerase was purchased from Stratagene (La Jolla, CA), and mutagenic primers were synthesized by Sigma Genosys (Oakville, ON, Canada). High Pure Plasmid Isolation kit was from Roche Diagnostics (Laval, QC, Canada). Source 15Q HPLC anion-exchange media and the Superose 12 FPLC gel filtration column were purchased from Amersham Pharmacia Biotech, Inc. (Baie d'Urfe, QC, Canada). Two-milliliter YM30 Centricon Centrifugal Filter devices were supplied by Millipore Corp. (Bedford, MA). All chemicals and media were from Fisher Scientific (Nepean, ON, Canada) or Sigma-Aldrich Co. (St. Louis, MO).

Plasmid Construction and Mutagenesis. pTFP1000 was hydrolyzed with Kpn I and Hind III producing two fragments, one containing thioredoxin−pepsinogen fusion gene (1.39 kb), which was isolated by agarose gel electrophoresis and extracted using a QIAquick gel extraction kit. This fragment was subcloned into pTrueBlue and transformed into *Escherichia coli* TOP10F' using the method of Hanahan (*11*). Transformed cells were plated on LB plates containing 100 μg/mL ampicillin and grown 16 h at 37 °C. White colonies were picked and cultured overnight in LB media to yield the plasmid pTBwt which served as the template to produce three mutants, E7K, T12A/E13Q, and E7K/T12A/E13Q using QuickChange Site-Directed Mutagenesis (Stratagene, La Jolla, CA). The following reverse and forward primers were designed for the single and double mutants using Gene Runner 3.00 software (Hastings Software Inc., Hastings on Hudson, NY):

E7K forward 5′GC GAT GAG CCC CTT AAG AAC TAC CTG G3′

E7K reverse 5′C CAG GTA GTT CTT AAG GGG CTC ATC GC3′

T12A/E13Q forward 5′ G AAC TAC CTG GAT GCG CAG TAC TTT GGC ACC 3′

T12A/E13Q reverse 5′ GGT GCC AAA GTA CTG CGC ATC CAG GTA GTT C 3′

Screening the isolated plasmids for the desired mutations was done by nucleotide sequencing using a T_7 promoter primer (Guelph Molecular Supercentre, University of Guelph, Guelph, ON, Canada). One mutated plasmid sample for each desired mutant was selected, cut with KpnI and HindIII and the fusion gene isolated as above. The isolated mutant fusion gene was then ligated back into pTFP vector, transformed into *E. coli* GI724. Cultures corresponding to correct mutant sequences were used to express thioredoxin−pepsinogen fusion protein.

Protein Expression and Purification. E. coli GI724 cultures containing wild-type and mutant pTFP1000 were used to innoculate 3 L induction medium (1XM9 salts, 0.2% casamino acids, 0.5% glucose, 1 mM $MgCl_2$, and 100 μg/mL ampicillin) and grown at 30 °C. Tryptophan was added to a final concentration of 150 μg/mL when the culture reached OD_{550} of 0.5, and was grown for an additional 8 h. The cells were pelleted by centrifugation at 6500*g* for 10 min, then resuspended with 100 mL of 20 mM Tris-HCl, pH 8.0. The cell suspensions were sonicated and cell debris removed by centrifugation at 35000*g* for 20 min, 4 °C. Ammonium sulfate was added to the supernatant to a final concentration of 10% saturation over 1 h on ice followed by centrifugation at 35000*g*, 20 min, 4 °C and the pellet was discarded. Additional ammonium sulfate was added to a final concentration of 40% saturation over 3 h, left at 4 °C overnight, then centrifuged as above. This pellet was resuspended in 5 mL of 20 mM Tris-HCl buffer, pH 8.0, followed by 4 × 1 L dialysis over 16 h at 4 °C. The desalted protein solution was applied to a 24-mL HR 10/30 Source Q HPLC column (Amersham Pharmacia Biotech, Inc., Baie d'Urfe, QC, Canada) and all samples and buffers for anion-exchange steps were in 20 mM Tris-HCl buffer, pH 8.0, and a flow rate of 2 mL/min. Initial removal of contaminating proteins was done using a 120 mL wash step followed by a 50 mL linear gradient from 10 to 260 mM NaCl. Thioredoxin−pepsinogen fusion protein was then eluted by increasing the salt concentration to 400 mM NaCl. Presence of pepsinogen in the fractions was identified by milk-clotting activity and Western blot using a polyclonal rabbit-anti-pepsinogen antibody produced in house. Thioredoxin-pepsinogen fusion protein fractions were concentrated in 2-mL YM30 Centricon centrifugal filter devices down to a final volume of less than 240 mL for subsequent gel filtration

[1] Abbreviations: E7K/T12A/E13Q: mutant porcine pepsin containing lysine, alanine, and glutamine in place of glutamate-7, threonine-12, and glutamate-13, respectively; WT: wild-type porcine pepsin; E7K: mutant porcine pepsin containing lysine in place of glutamate-7; T12A/E13Q: mutant porcine pepsin containing alanine and glutamine in place of threonine-12 and glutamate-13, respectively; pTFP1000: thio fusion protein plasmid purchased from Invitrogen (Carlsbad, CA) containing the porcine pepsinogen gene fused to the 3′-end of the thioredoxin gene; Ip: pepsin structural intermediate existing at pH 7.2 and 8.0; Iap: proposed structural intermediate existing between native pepsin and Ip; Np: native pepsin.

using a Superose 12 FPLC column (Amersham Pharmacia Biotech, Inc., Baie d'Urfe, QC, Canada) using a flow rate of 0.5 mL/min and 20 mM Tris-HCl buffer, pH 8.0. Fractions containing the fusion protein were identified, concentrated, and gel filtered as above two additional times to attain purity, as determined by silver-stained SDS−PAGE. Glycerol was added to the pure pepsinogen fusion protein samples to a final concentration of 50% w/w and stored at −25 °C. The enzyme samples were activated in a pH 1.0 buffer and the prosegment was removed by gel-filtration, 30 kDa exclusion limit.

Protein Concentration Determination. Enzyme concentrations for kinetic assays and pH studies were determined by pepstatin titration (*10*). Protein concentration determinations for the purification steps and circular dichroism spectroscopy were carried out using a Coomassie protein microassay as per Pierce (Rockford, IL). Standard dilutions of commercially obtained porcine pepsinogen were used to generate standard curves.

K_m and k_{cat} Determinations. Kinetic parameters were determined using a standard room-temperature assay for the cleavage of the chromophoric octapeptide, KPAEFF(NO_2)AL, in the presence of 0.22 pmol enzyme in a total reaction volume of 100 μL, 100 mM sodium citrate buffer, pH 2.6 (10). The decrease in absorbance at 300 nm was recorded for 3 min and the initial rate ($-\Delta A$/min) was determined by calculating the slope of the linear portion of the data points. Each sample was done in triplicate for each substrate concentration. A conversion factor specific to the substrate used, 1.35 OD/mM, was divided into the initial rate and directly plotted against substrate concentration using nonlinear regression to obtain K_m and k_o (*10*). All data were also analyzed using Woolf-Hanes plots to confirm the nonlinear-derived values.

SDS−PAGE and Electroblotting. The method of Laemmli (*12*) was followed using a Bio-Rad Mini Protean II electrophoresis apparatus (Bio-Rad Laboratories), 12.5% acrylamide gels, and 100 V.

Far-UV Circular Dichroism Spectropolarimetry. Far-UV circular dichroism spectra were determined from 250 to 190 nm at room temperature in a 200 μL quartz cuvette with a 0.1-cm path length using a Jasco J-600 spectropolarimeter (Japan Spectroscopic Co., Ltd., Tokyo, Japan). The average of four scans were taken for zymogen and active samples, and buffer spectra were subtracted from the average sample spectra. Zymogens were scanned in 20 mM Tris-HCl buffer, pH 7.5, at concentrations between 0.1 and 0.2 mg/mL. Active samples were scanned within the same concentration range in 20 mM sodium acetate buffer, pH 5.3. Molar ellipticity was calculated from the observed degrees ellipticity and the mean residue weight of 107 for pepsin using the method of Yada and Nakai (*13*). Molar ellipticity versus wavelength plots were compared for each pepsin form.

A circular dichroism time-course study for the denaturation of wild-type and mutants at pH 7.0, 25 °C, was also done. A total of 120 μL of active enzyme were mixed with 60 μL of 60% w/v glycerol/300 mM sodium phosphate buffer, pH 7.0. Single scans were started at $t = 0$, 4, 8, 12, 16, 20, 30, and 40 min, while the denaturation incubations proceeded. For each spectrum, the beginning of the scan (250 nm) occurred at the times listed above, and proceeded at 20 nm/min. The time corresponding to any given wavelength during the scans was $t_{start} + [(250\text{ nm}-\lambda)/20\text{ nm/min}]$. The measured baseline spectrum for a solution of 120 μL of 20 mM sodium acetate buffer, pH 5.3 and 60 μL of 60% w/v glycerol/300 mM sodium phosphate buffer, pH 7.0 was subtracted for the denaturation scans as the blank correction. Further CD investigation of the relative denaturation processes of wild-type and mutant E7K/T12A/E13Q was done using the same conditions as above by measuring ellipticity at a fixed wavelength, 222 nm.

pH Stability. Time for wild-type and mutant enzymes to be inactivated at pH 7.0 was determined by the following protocol: 15 μL of 500 nM active enzyme were added to 60 μL of 25% w/v glycerol/500 mM potassium phosphate buffer, pH 7.0 (final concentrations 100 nM enzyme, 20% w/v glycerol, 400 mM potassium phosphate buffer, pH 7.0). Proteolytic activity was assessed over time using the assay described above (K_m and k_{cat} determinations). Five microliter aliquots of incubating sample were removed every 3 min through $t = 21$ min, then every 4 min until no activity was detected for three consecutive readings. Activity was expressed as percent residual activity relative to the activity corresponding to $t = 0$.

pH Dependence of Activity. The proteolytic activity of wild-type and mutants were determined by a method adapted from (*10*) at the following pH values: 0.9, 1.6, 2.1, 2.6, 3.0, 3.5, 3.9, 4.4, 5.0, 5.6, 5.9, and 6.5. Activity was determined using reaction conditions of 90 mM sodium citrate buffer, 6−9 nM enzyme, 100 μM KPAEFF(NO_2)AL chromophoric octapeptide substrate (*14*), 100 μL total reaction volume at room temperature. All observed rates were calculated from the linear decay in absorbance at 300 nm and the specific activities were expressed relative to the highest activity for the respective samples.

pH Dependence of Activation and Activation of Fusion Protein Zymogens. Determination of pH dependence of activation for wild-type and mutants were determined at pH 1.0, 2.0, 3.0, 3.5, 4.0, 4.5, and 5.0. Five microliters of 1 μM zymogen fusion protein solution was mixed with 15 μL of 133 mM sodium citrate buffer (100 mM citrate concentration final) for 5 min at room temperature. The amount of activation was determined by assessing proteolytic cleavage of the synthetic peptide substrate described above (K_m and k_{cat} determinations). Cleavage rates were expressed as percent relative activity, relative to the highest rate obtained for each sample.

Molecular Modeling. Molecular models of wild-type and mutant pepsinogen forms were determined using the crystal structure coordinates of porcine pepsinogen (1PSG) and the modeling program Insight II (Accelrys Inc., San Diego, CA). Energy minimization was done for 20 000 iterations with maximum derivatives of 4.18 kJ mol^{-1} and a constant valence force field for each atom calculated up to 24 Å.

RESULTS

Protein Isolation. Thioredoxin−pepsinogen fusion protein, expressed in *E. coli*, was isolated and purified using ammonium sulfate precipitation, dialysis, anion-exchange HPLC, and gel-filtration HPLC. Sample purity was evidenced by a single peak on gel filtration elution profiles, a single band on silver-stained SDS−PAGE, and a final purification factor of 2500 (data not shown). Pure fusion protein samples were stored in 20% glycerol/80% 20 mM Tris-HCl, pH 8.0, at −20 °C to preserve activity.

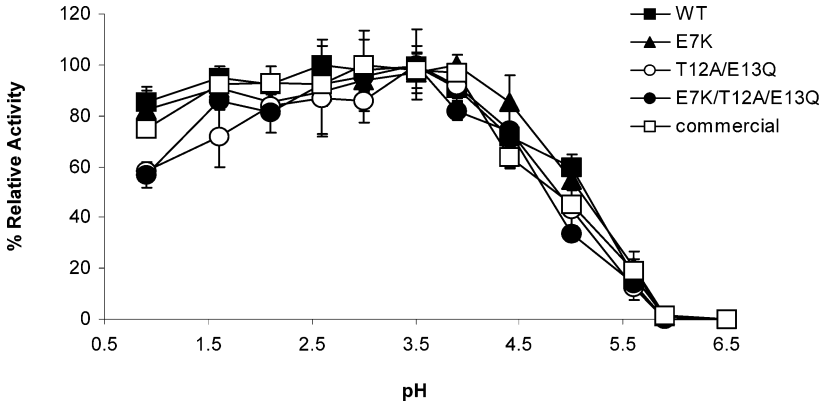

FIGURE 1: pH dependence of activity profile for the various pepsin forms: Activity was assayed using 100 μM chromophoric substrate KPAEFF(NO_2)AL, 95 mM sodium citrate buffer, RT, and 6−9 nM enzyme.

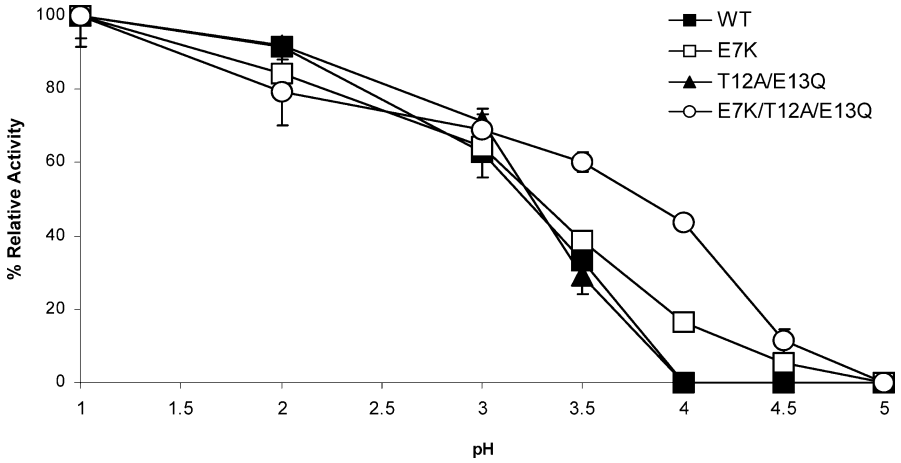

FIGURE 2: pH dependence of activation of the zymogen fusion protein samples: Activation reactions contained 250 nM protein, 100 mM sodium citrate buffer, and were incubated at 25 °C. Activity was assessed after exactly 5 min activation time using 12.5 nM enzyme and 100 μM chromophoric substrate KPAEFF(NO_2)AL. Activity is shown as percent relative activity with respect to the highest rate obtained for the respective pepsin forms.

pH Dependence of Activity. pH dependence of activity for WT, commercially obtained porcine pepsin, and the three mutants of the present study was determined over a broad range of pH values (Figure 1). WT recombinant pepsin showed highest activity at pH 2.6 and displayed greater than 90% activity over the pH range 1.6−3.9. Results for WT were similar to those reported previously using the same synthetic substrate (*10*, *16*). Also, the pH−activity profile of recombinant WT was similar to that for commercially obtained porcine pepsin.

The pH−activity profiles of WT and the three mutants were similar overall, with the exception of significantly lower activities for mutants T12A/E13Q and E7K/T12A/E13Q, relative to WT, at pH 0.9 ($P \leq 0.05$, respectively). Since the former two mutants contained mutations at positions 12 and 13, it appeared that Thr12 and/or Glu13 were important for catalysis of the peptide hydrolysis reaction under extremely low pH conditions, whereas the introduction of positively charged Lys at position 7 in place of Glu had no observable effect.

pH Dependence of Activation. The pH dependence of activation of the fusion protein zymogens was determined by incubation at various acidic pH values followed by immediate proteolytic assay as the means of detecting the relative degree of activation. Proteolytic assays were carried out at pH 5.3 as no activation was detected for the various pepsin forms at this pH (data not shown). The results are shown in terms of percent relative activity resulting from activation at pH values between pH 1.0 and 5.0 (Figure 2). Activation of WT was detected for pH values below 4.0 in the 5 min time period used in the activation study, in agreement with Richter et al. (*17*). WT displayed the highest amount of activation at pH below 2.0, and sharply decreased at pH above 3.0, similar to the results of Tanaka and Yada (*18*). T12A/E13Q showed nearly identical activation results compared to WT (Figure 2). By contrast, both E7K and E7K/T12A/E13Q were activated at pH 4.0 and 4.5, suggesting that the introduction of Lys at position 7 was responsible for the observed differences.

Binding, Catalysis, and Specificity. Kinetic parameters of WT and the three mutant pepsin forms were determined by nonlinear regression analyses. The K_m and k_{cat} values are summarized in Table 1. Two data groupings were noted: T12A/E13Q and E7K/T12A/E13Q had similar K_m values ($P > 0.05$), while those for WT and E7K were similar ($P > 0.05$). The higher K_m values of the former grouping were significantly different from those of the latter grouping ($P \leq 0.05$). The turnover numbers for E7K and E7K/T12A/E13Q were similar ($P > 0.05$), lower than that for WT ($P \leq 0.05$) and greater than that for T12A/E13Q ($P \leq 0.05$).

pH Inactivation. WT, E7K, T12A/E13Q, and E7K/T12A/E13Q were incubated in 400 mM sodium phosphate buffer, pH 7.0, containing 20% glycerol. Residual activity was determined at pH 2.6, and results were expressed as percent

Table 1: Summary of the Kinetic Parameters Obtained by Nonlinear Regression Using the Method of Least-Squares for Best Fit to the Michaelis−Menten Model[a]

	K_m (μM)	k_{cat} (s^{-1})	k_{cat}/K_m (μM^{-1} s^{-1})
WT	70 ± 10	98 ± 7	1.4
E7K	100 ± 20	65 ± 6	0.65
T12A/E13Q	190 ± 30	42 ± 4	0.22
E7K/T12A/E13Q	190 ± 28	76 ± 7	0.39

[a] All values were obtained by averaging determinations done in triplicate at pH 2.6.

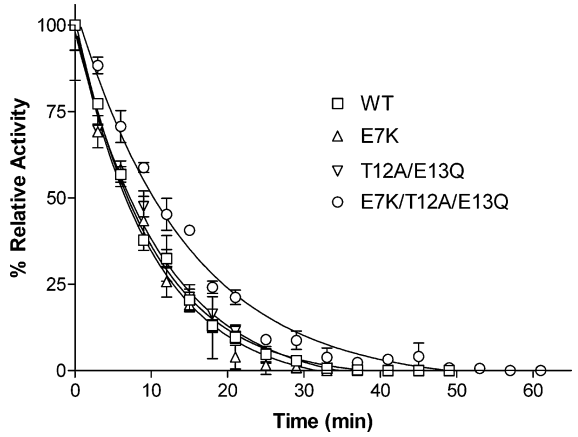

FIGURE 3: pH-inactivation of WT and mutants: Percent relative residual activity is shown for 100 nM active pepsin samples incubated at RT in 400 mM sodium phosphate buffer, 20% glycerol, pH 7.0. Residual activity was measured using 100 μM chromophoric substrate KPAEFF(NO_2)AL, 95 mM sodium citrate buffer, pH 2.6, and 5 nM enzyme.

relative activity, relative to initial activity (Figure 3). The pH 7.0 incubation times required for inactivation were similar for WT, E7K, and T12A/E13Q. Nonlinear regression analyses were done for exponential decay equations fitted to the inactivation data. The rate constants and standard errors for the exponential decay of WT, E7K, T12A/E13Q, and E7K/T12A/E13Q were 0.10 ± 0.004, 0.098 ± 0.008, 0.087 ± 0.006, and 0.069 ± 0.005 min^{-1}, respectively. The rates of activity loss for E7K and T12A/E13Q relative to WT were not significantly different ($P > 0.05$), whereas E7K/T12A/E13Q lost activity significantly slower than WT ($P \leq 0.05$). The improved stability, unique to the triple mutant, suggested a synergistic effect of the three N-terminal mutations.

Structural Effects of the Mutations. The far-UV CD spectra of both the zymogenic fusion protein and mature pepsin forms were determined at pH 7.0 and 5.3, respectively, to determine if the mutations resulted in major secondary structure changes under nondenaturing conditions. For each sample, four scans were collected and averaged (data not shown). The overall shape of the four zymogen spectra were similar, revealing no apparent differences in secondary structure. In addition, no differences were apparent among the mature pepsin spectra.

Since differences in the rates of inactivation were detected upon incubation at pH 7.0, and pH-induced denaturation of pepsin involves unfolding of the enzyme structure, including loss of secondary structural elements (*19*), it was predicted that the rate of denaturation could be differentially detected for the pepsin forms, and such structural changes should coincide with loss of function. To investigate secondary structural changes during the denaturation process, the far-UV CD spectra of WT and the three mutants were obtained for samples incubated at pH 7.0 over a 40 min period (data not shown). Inspection of the neutral-pH, far-UV CD scans for all samples revealed a broadening of the overall spectral shape as denaturation proceeded and all spectra exhibited a blue-shift in the 208−198 nm region over time. For WT, E7K, and T12A/E13Q, a large spectral shift occurred during the initial 4 min and relatively rapid spectral change proceeded up until 12 min. The 20, 30, and 40 min scans were essentially constant, an indication that changes in secondary structure at pH 7.0 was complete. Distinct changes in the E7K/T12A/E13Q far-UV CD scans were apparent in that the initial scans were overlapping and the later scans were nonsuperimposable, indicating constant secondary structural changes throughout the 40 min period.

To quantify differences in secondary structural changes, the scans corresponding to the various denaturation times were subtracted from the respective $t = 0$ scans yielding difference spectra. Areas under the difference spectra were calculated, thus providing an estimate of the total amount of spectral change. Amount of spectral change was then normalized to give the proportion of remaining spectral change at given denaturation times using the equation $[(1 - A/A_{max}) \times 100]$. The normalized data were plotted against denaturation time and compared to the inactivation curves for WT and E7K/T12A/E13Q, the mutant that exhibited better retention of activity (Figure 4). The changes in secondary structure were similar to the loss of residual activity at pH 7.0 for the respective pepsin forms. For example, after a 20 min incubation at pH 7.0, 87% of total spectral change, and approximately 90% activity loss, were observed for WT. For E7K/T12A/E13Q, 85% of the total area change, and approximately 90% activity loss, were observed at 30 min. The data over 40 min were fitted to an exponential decay equation using nonlinear regression. For WT, the rate constant for the decay in remaining spectral change (0.093 ± 0.004 min^{-1}) was not significantly different from the rate of decay in residual activity (0.095 ± 0.005 min^{-1}) ($P > 0.05$). Likewise for E7K/T12A/E13Q, the rate constants for remaining spectral change (0.042 ± 0.005 min^{-1}), and activity loss (0.054 ± 0.006 min^{-1}), were not significantly different ($P > 0.05$). The WT and mutant data sets were significantly different from each other ($P \leq 0.05$). These data demonstrated that the inactivation of pepsin was associated with the conversion of native pepsin to a pH 7.0 denatured structure and such structural change occurred slower for E7K/T12A/E13Q compared to WT. It followed that the better retention of function of E7K/T12A/E13Q was related to the N-terminal mutations. Additionally, the above application of CD spectropolarimetry, together with its analysis methodology, represented a novel use of this technique in the study of structure−function relationships among aspartic proteinases.

To further explore the use of far-UV CD as applied to the kinetics of pepsin denaturation, the mutants were compared to WT at a fixed wavelength, 222 nm, at pH 7.0 over a 60 min time period. The ellipticity data were normalized and expressed as percent molar ellipticity change remaining, relative to the maximum observed ellipticity data point and compared to the pH-inactivation results (Figure 5). An increase in intensity at 222 nm was observed for E7K and E7K/T12A/E13Q, while the variation in the WT and T12A/

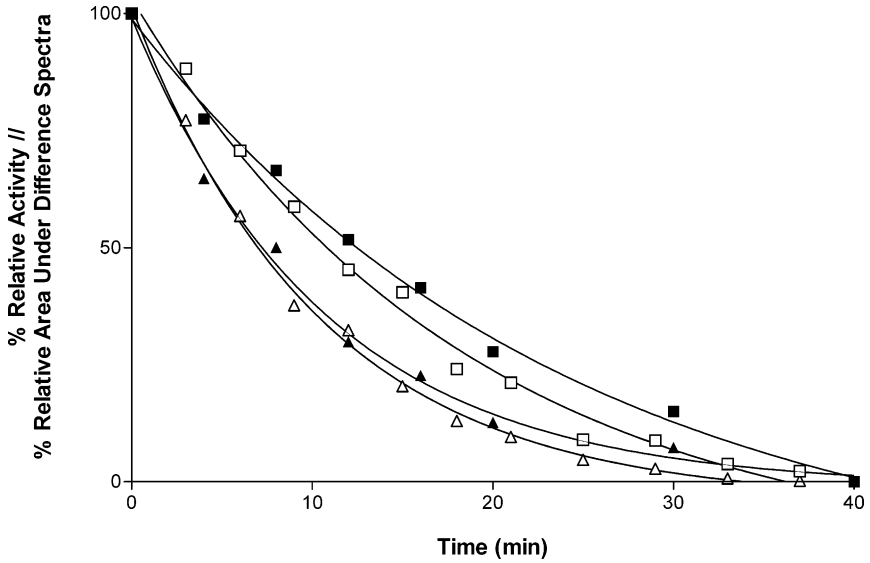

FIGURE 4: Comparison of CD spectral change and activity loss: Area under the far-UV CD difference spectra for WT (solid triangles) and E7K/T12A/E13Q (solid squares) are shown as normalized percent relative values. The CD spectra for WT and mutants were collected at various denaturation times using a Jasco J-600 spectropolarimeter. Activity loss at pH 7.0 is shown as percent relative residual activity for WT (open triangles) and E7K/T12A/E13Q (open squares). Residual activity was assessed using 100 μM chromophoric substrate KPAEFF(NO_2)AL, 95 mM sodium citrate buffer, pH 2.6, and 5 nM enzyme. There were no significant differences ($P > 0.05$) in the exponential rate constants for CD spectral change and inactivation of WT and E7K/T12A/E13Q, respectively.

E13Q data were not significantly different from that of the buffer control ($P > 0.05$). For E7K/T12A/E13Q, the rates of decay in molar ellipticity change remaining and activity loss at pH 7.0 were 0.085 ± 0.01 and 0.069 ± 0.004 min^{-1}, respectively ($P > 0.05$). For E7K, the rate of molar ellipticity change remaining and activity loss were 0.11 ± 0.01 and 0.098 ± 0.008 min^{-1}, respectively ($P > 0.05$). The data indicated that structural changes in the single and triple mutants were occurring at similar rates to those for the loss of function. Additionally, the increase in 222 nm signal was retained by E7K and E7K/T12A/E13Q, indicating a permanent change in secondary structure under neutral conditions.

Further structural investigation employed molecular modeling to predict alpha-carbon movement in the mutant pepsin forms relative to wild-type porcine pepsin. Differences were revealed on plots of largest alpha-carbon movement versus residue number, indicative of flexibility changes within the mutant structures (data not shown).

DISCUSSION

Activation of pepsinogen begins with a conformational change in the proenzyme segment that is induced by protonation of carboxyl side-chains under acidic conditions (*2*). Four pH-sensitive, ion-paired interactions between the enzyme body and prosegment are Asp11−Arg13p, Glu13−Arg8p, Asp3−His29p, and Glu7−His31p (*1*, *2*). The observation that E7K and E7K/T12A/E13Q activated at higher pH indicated that Glu7, and its interaction with His31p, are important to the activation process. Activation of WT and T12A/E13Q was restricted to pH below 4.0, whereas activation occurred above pH 4.0 for the two mutants which contained positively charged Lys in place of Glu7. This contribution to pH-regulation of activation suggested that protonation of Glu7 occurs close to pH 4, consistent with the normal pK_a of glutamate. The observation that mutation of Glu7 resulted in a larger effect on the activation process compared to Thr12/Glu13 agreed with the relatively high strength of the Glu7−His31p interaction (*2*). E7K/T12A/E13Q activated faster than E7K at pH 3.5 (Figure 2), suggesting that the two affected prosegment-enzyme interactions, 7−31p and 13−18p, had an additive effect to pH-control of activation.

Differences in pH dependence of activity were observed for mutants T12A/E13Q and E7K/T12A/E13Q (Figure 1). In wild-type, Leu10−Thr12 and Asp11−Asp159 are the only two hydrogen-bonding pairs in the Tyr9−Glu13 turn region. At very low pH, the side-chain-backbone Asp11−Asp159 interactions are eliminated due to the protonation of the carboxyl side-chains, thereby leaving the pH-insensitive Thr12−Leu10 hydrogen bond as the lone interaction responsible for proper orientation of the Tyr9−Glu13 turn. In T12A/E13Q and E7K/T12A/E13Q, the Thr12−Leu10 hydrogen bond is not possible due to the inability of the mutant Ala12 side-chain to hydrogen bond. The Tyr9−Glu13 turn has been suggested to be critical to substrate binding due to its proximity to the substrate binding cleft (*9*). It is thus postulated that the disruption of the Asp11−Asp159 interactions at low pH resulted in destabilization of the 9−13 turn.

The K_m and k_{cat} values obtained for WT were in agreement with previously published values for pepsin using the same synthetic substrate (*7*, *16*, *17*, *21*), and similar to those reported for a substrate differing only at the P_2' position (*22*). It was previously determined that residues of the 9−13 loop were not involved in pepstatin binding (*23*), and that E13A pepsin had normal activity on substrate containing a hydrophobic residue at the P_3 position (*24*). The present study indicated a lowered specificity constant and binding affinity for mutants T12A/E13Q and E7K/T12A/E13Q using a similar, hydrophobic P_3 substrate (Table 1). Thr12 was previously implicated as being involved in substrate binding (*1*), and structurally it is part of a turn in which the polypeptide changes direction between the Glu7−Tyr9 β-strand and the Glu13−Gly16 β-strand (*9*). Thus, the present study suggested that Thr12 is important to substrate

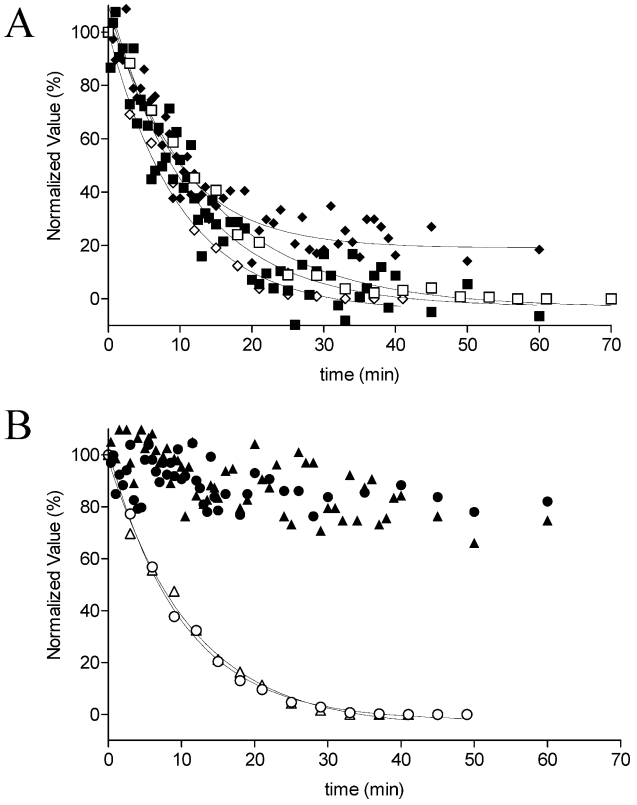

FIGURE 5: Comparison of normalized molar ellipticity change at 222 nm and activity loss: Molar ellipticity change for WT and mutants incubated in 100 mM sodium phosphate buffer, pH 7.0, 20% glycerol, RT, was monitored at 222 nm using a Jasco J-600 spectropolarimeter and a 200 μL cell. Activity loss at pH 7.0 is shown as percent relative residual activity, assayed with 100 μM chromophoric substrate KPAEFF(NO_2)AL, 95 mM sodium citrate buffer, pH 2.6, and 5 nM enzyme. (A) The rate of 222 nm molar ellipticity change (E7K; solid diamonds, E7K/T12A/E13Q; solid squares) and activity loss (E7K; open diamonds, E7K/T12A/E13Q; open squares) were not significantly different ($P > 0.05$) for the respective mutants. (B) The lack of a relationship between 222 nm molar ellipticity change (WT; closed circles, T12A/E13Q; closed triangles) and activity loss (WT; open circles, T12A/E13Q; open triangles) is shown for WT and T12A/E13Q. 222 nm molar ellipticity for WT and T12A/E13Q did not vary with time linearly or nonlinearly in a significant fashion.

affinity through its role in positioning the 9−13 loop. It also supported the concept of amino acid residues apart from the catalytic center can be important for binding and catalysis despite a lack of direct interaction with substrate (*16*, *25*).

All three mutants yielded reduced turnover relative to wild-type. E7K and E7K/T12A/E13Q yielded similar turnover numbers, while T12A/E13Q had the lowest k_{cat} (Table 1). Mutations at positions 12 and 13 were detrimental to turnover, yet such effects were apparently less severe when coupled with mutation of Glu7. Distortions within this region of pepsin could diminish the turnover ability due to the proximity of the mutations to the Tyr14−Phe31 and Gly16−Val29 hydrogen bonds, the only intrasheet interactions between the Glu13−Gly16 strand and the Val29−Asp32 strand (*9*). Misalignment of Asp32, one of the catalytic Asp residues, would be expected to detrimentally affect catalysis (*26*). Greater flexibility of the E7K/T12A/E13Q N-terminus and the neighboring Glu13−Gly16 strand may help to minimize strain caused by unfavorable interactions at mutant residues 12 and 13.

The initial step of inactivation has been shown to be the denaturation of the N-terminus from the enzyme body caused by electrostatic repulsion between deprotonated N-terminal residues (*6*, *7*). Conformational changes evidenced by increases in 222 nm ellipticity during denaturation, and the corresponding activity loss (Figure 5), suggested that the triple mutant N-terminus inhibited the native to inactive intermediate conformational transition. For the E7K/T12A/E13Q N-terminus to protect the active site, the acid-pH β-structure of the Gly2−Tyr14 pepsin segment is required to rearrange either to a coil, as observed for the Tyr10 and Lys8 segments of cathepsin D (*8*), or to a helix as observed for pepsinogen segments encompassing Tyr9 and Lys36p during activation (*3*). The required rearrangement in mutant pepsin was thought possible since the segment Gly2−Tyr14 comprises a helical structure at neutral pH in the zymogenic form of pepsin, and therefore, would revert to such conformation from its acid-pH β-strand, especially upon introduction of the cathepsin D-like mutations. The observed increase in CD intensity at 222 nm was consistent with such a structural rearrangement.

Molecular modeling revealed that among the regions of the mutant pepsin molecules that showed increased flexibility were segments Tyr44−His53 and Ser104−Phe117, both proximate to the N-terminus. The structural equivalents of these pepsin regions in cathepsin D are His45−His56 and Ala118−Phe131, respectively, and both are noted for their large conformational change upon incubation at neutral pH accompanying the relocation of the N-terminus into the active site (*8*). For a stabilizing structural mechanism similar to that employed by cathepsin D to work in mutant pepsin, it was expected that homologous structural rearrangements would be required, thus the mutant pepsin models provided further support to the hypothesis that the N-terminal mutations engineered into pepsin resulted in a protective structural mechanism against neutral pH-denaturation.

The changes observed for the far-UV CD spectrum of pH 7.0 denatured pepsin were in agreement with Yada and Nakai (*13*), and contrasted previous CD results at pH 7.2 (*19*) and pH 8.0 (*27*). The pH 7.2 denatured pepsin gave a similar spectrum to that reported for pH 8 pepsin (Ip). Both the pH 7.2 (*19*) and pH 8.0 (*27*) denatured forms showed an approximate 60% increase in intensity at 206 nm (the local minimum of the denatured spectrum) and a large loss of intensity for the 225−212 nm spectral region. pH 7.0 denatured pepsin showed only 32% increase in intensity at 206 nm, and no large change in the 225−210 nm region. Overall, a blue-shift in the region below 210 nm was consistent among the above CD-denaturation studies, characteristic of random coil structure. The far-UV CD results of the present study supported the conclusion that partially unfolded, inactive pepsin intermediate (Ip) retained substantial secondary structural elements (*27*). However, pH 7.0 denatured pepsin retained more secondary structure in comparison to the pH 7.2, or pH 8.0, denatured forms and the extent of secondary structural denaturation required to inactivate pepsin was substantially less than the structural changes observed at higher pH. The pH 7.0 spectrum resembled that for denatured pepsin upon re-acidification to pH 5.4 (*19*). Taken together, the CD and inactivation results suggested the existence of another pepsin intermediate (Iap) between the native form (Np) and the pH 7.2, or 8.0,

denatured form (Ip). Thus, the structural changes occurring between Iap and Ip were apparently reversible, unlike the secondary structural transitions occurring between Np and Iap. Further study using DSC and NMR will allow the characterization of the energetic, and structural, transition from Iap to Ip.

In conclusion, elimination of the carboxyl-containing side-chains at positions 7 and 13, individually, or the introduction of an N-terminal positive charge, did not produce any significant differences in inactivation rate upon lowering pH. The observed synergistic effect of all three mutations at positions 7, 12, and 13 to increase neutral pH stability suggested a mode of action not solely dependent on ionizable carboxylate groups and also supports the findings of Tanaka and Yada (*7*) who suggested that restriction of N-terminal movement retards denaturation.

ACKNOWLEDGMENT

We would like to thank Dr. Alejandro Marangoni for his advice regarding data analysis and Dr. Massimo Marcone for his help with CD spectropolarimetry.

REFERENCES

1. Sielecki, A. R., Fedorov, A. A., Boodhoo, A., Andreeva, N. S., and James, M. N. G. (1990) *J. Mol. Biol. 214*, 143−170.
2. James, M. N. G., and Sielecki, A. R. (1986) *Nature 319*, 33−38.
3. Sielecki, A. R., Fujinaga, M., Read, R. J., and James, M. N. G. (1991) *J. Mol. Biol. 219*, 671−692.
4. Rahuel, J., Priestle, J. P., and Grutter, M. G. (1991) *J. Struct. Biol. 107*, 227−236.
5. Bohak, Z. (1969) *J. Biol. Chem. 244*, 4638−4648.
6. Lin, X.-l., Loy, J. A., Sussman, F., and Tang, J. (1993) *Protein Sci. 2*, 1383−1390.
7. Tanaka, T., and Yada, R. Y. (2001) *Protein Eng. 14*, 669−674.
8. Lee, A. Y., Gulnik, S. V., and Erickson, J. W. (1998) *Nat. Struct. Biol. 5*, 866−871.
9. Cooper, J. B., Khan, G., Taylor, G., Tickle, I. J., and L., B. T. (1990) *J. Mol. Biol. 214*, 199−222.
10. Tanaka, T., and Yada, R. Y. (1996) *Biochem. J. 315*, 443−446.
11. Hanahan, D. (1983) *J. Mol. Biol. 166*, 557−580.
12. Laemmli, U. K. (1970) *Nature 227*, 680−685.
13. Yada, R. Y., and Nakai, S. (1986) *J. Food Biochem. 10*, 155−183.
14. Fusek, M., Lin, X.-l., and Tang, J. (1990) *J. Biol. Chem. 265*, 1496−1501.
15. Kervinen, J., Sarkkinen, P., Kalkkinen, N., and Saarma, M. (1993) *Phytochemistry 32*, 799−803.
16. Cottrell, T. J., Harris, L. J., Tanaka, T., and Yada, R. Y. (1995) *J. Biol. Chem. 271*, 19974−19978.
17. Richter, C., Tanaka, T., Koseki, T., and Yada, R. Y. (1999) *Eur. J. Biol. 261*, 746−752.
18. Tanaka, T., and Yada, R. Y. (1997) *Arch. Biochem. Biophys. 340*, 355−358.
19. Favilla, R., Parisoli, A., and Mazzini, A. (1997) *Biophys. Chem. 67*, 75−83.
20. Topol, I., Cachau, R., Burt, S., and Erickson, J. (1995) in *Adv. Exp. Medic. Biol.* (Takahashi, K., Ed.) Vol. 362, pp 549−554, Plenum Press, New York.
21. Okoniewska, M., Tanaka, T., and Yada, R. Y. (2000) *Biochem. J. 349*, 169−177.
22. Rao, C. M., and Dunn, B. M. (1995) in *Adv. Exp. Medic. Biol.* (Takahashi, K., Ed.) Vol. 362, pp 91−94, Plenum Press, New York.
23. Fujinaga, M., Chernaia, M. M., Tarasova, N. I., Mosimann, S. C., and James, M. N. (1995) *Protein Sci. 4*, 960−972.
24. Rao, C. M. (1994) in *A Detailed Investigation into the Enzymatic Specificity of Porcine Pepsin*, Ph.D. Thesis, University of Florida, Gainsville, Florida.
25. Park, Y., Nishiyama, M., Horinouchi, S., and Beppu, T. (1995) in *Adv. Exp. Medic. Biol.* (Takahashi, K., Ed.) Vol. 362, pp 559−563, Plenum Press, New York.
26. Aikawa, J., Park, Y. N., Sugiyama, M., Nishiyama, M., Horinouchi, S., and Beppu, T. (2001) *J. Biochem. (Tokyo) 129*, 791−794.
27. Konno, T., Kamatari, Y. O., Tanaka, N., Kamikubo, H., Dobson, C. M., and Nagayama, K. (2000) *Biochemistry 39*, 4182−4190.

BI0348112